FROM DEBRIS IN LAKE SEDIMENTS TO BACK-CALCULATION OF SNOW AVALANCHES ON LAKE ICE OF ANESTØLSVATNET, NORWAY

Denise Rüther[1]*, Torgeir Opeland Røthe[1] and Simon de Villiers[1]

[1] *Western Norway University of Applied Sciences, Sogndal, Norway*

ABSTRACT: Situated at 439 m a.s.l. in northernmost Sogndalsdalen, Western Norway, lake Anestølen has a known history for snow avalanches which primarily originate from the mountain to the west, Oksli (Figure 1a). Previous work based on the analyses of ten short sediment cores, taken in a west-east transect across lake Anestølen, gives a historical perspective to snow avalanche activity. We can distinguish two lake sediment signatures derived from snow avalanches: (i) the first sedimentary unit SA1 is attributed to snow avalanche debris melting out from lake ice and (ii) the second sedimentary unit SA2 is suggested to form by snow avalanches which break through lake ice. A local farmer who has performed regular control measurements of snow depth and density since 2011 has observed two larger snow avalanches in the past years. Whilst occurring in the same avalanche path, the snow avalanches had markedly different characteristics. The one observed in 2012 had relatively long runout on the frozen lake surface, while the one observed in 2015 broke the lake ice, piled up at proximity to the western lake shore and caused shore-parallel fractures all the way across the lake. We explore the weather conditions contributing to the two known events. Further the observed maximum runout based on the sediment cores and the 2012 avalanche have been back-calculated with the help of RAMMS::Avalanche and RAMMS::Extended. Notably RAMMS::Avalanche does not produce long enough runouts to match our observations. Finally, observations and RAMMS scenarios are discussed focusing on the performance of the models and whether lake ice with different thicknesses may break in various scenarios.

KEYWORDS: snow avalanches on lake ice, lacustrine record, avalanche modelling

1. INTRODUCTION

Snow avalanches occur regularly in mountainous polar and subpolar regions impacting frozen water bodies where avalanche tracks extend onto lakes or fjords. Yet, this process is relatively poorly documented and to our knowledge no published studies have explored how to best model these scenarios. The only account that we are aware of occurred during a mass movement cycle in July 2022 in New Zealand (Miller et al., 2023) when two snow avalanches hit newly formed ice on Hooker lake. In this study, we take observations of snow-avalanche-transported sediment debris in lake sediments and direct observations of historical avalanches as starting point to back-analyze known runouts with RAMMS::Avalanche and RAMMS::Extended and explore under which conditions lake ice may break due to snow avalanche impact.

2. SNOW AVALANCHE SIGNATURE IN LACUSTRINE SEDIMENTS

Lake Anestølen (Anestølsvatnet in Figure 1a) and its surroundings are valuable archives for mass movement activity as shown in three student theses from the 1990s which are summarized in Aa et al. (2022). Despite extensive research over the past decades, correlation of mass movement events across core locations remained difficult. Therefore, ten short sediment cores with undisturbed top were retrieved and analyzed by two groups of students in 2017/18 (Kimerud and Hansen, 2018; Bergaas et al., 2018). The focus of these bachelor theses was to explore shallow landslide induced turbidites and snow avalanche deposits in lakes in greater detail. Building on this work Rüther et al. (2024) have prepared a manuscript to be submitted to the journal Sedimentology. We found that minerogenic clasts with diameters greater than 2 mm, often in combination with organic clasts, at the lake floor more than ten-meter distance from the lake shore can be seen as evidence for snow avalanches on a frozen lake surface. We observe eight snow-avalanche-lithofacies, mostly diamicts, which are distinguished based on the content and size of organic and minerogenic clasts as well as sedimentary structures. These eight lithofacies are further grouped into two categories (1) unit SA_1 for snow avalanches that hit a frozen lake surface and melt out in late spring to summer and (2) unit SA_2 for snow avalanches that broke the lake ice surface so that any soil or minerogenic grains were then deposited from a turbulent mixture of water, snow and loose material. Snow avalanche event layers belonging to unit SA_2 are found in the three westernmost cores, whereas unit SA_1 is observed in all

* *Corresponding* author address:
Denise Rüther, Western Norway University of Applied Sciences, Røyrgata 6, 6856 Sogndal, Norway;
tel: +47 57 67 76 29; email: denise.christina.ruther@hvl.no

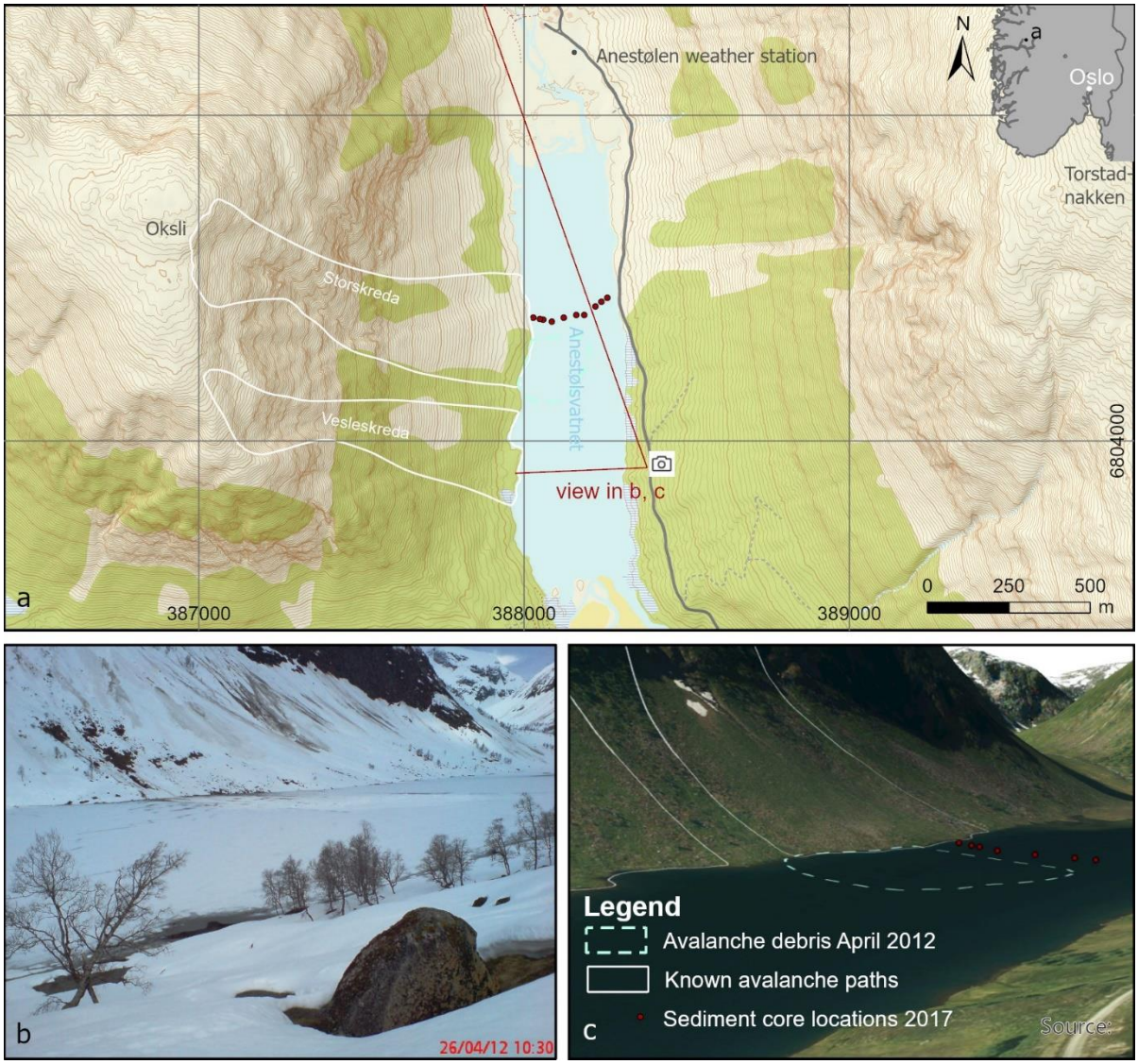


Figure 1: Location map showing the lake Anestølen in western Norway (**a**), photo taken på Ottar Husum on April 26th, 2012 (**b**), and three-dimensional view of an aerial photo from 2018 (**c**) showing lake Anestølen at similar angle as the photo shown in b.

but the three easternmost cores (Figures 1a and 4). The absence of any avalanche debris in the eastern cores supports more recent observations which suggest that snow avalanches are more seldom from the eastern mountain Torstadnakken (Figure 1a) and do not tend to have runouts onto the lake. Notably, we interpret the occurrence of snow avalanche debris in sediment cores as maximum runouts from the mountain Oksli. Therefore, we make the assumptions that avalanches from Torstadnakken can be neglected and that lake ice with avalanche debris does not drift significantly before it melts.

3. METHODS

The Norwegian Water and Energy Directorate (NVE) maintains an automated weather station measuring precipitation, air temperature, snow water equivalent and snow depth at Anestølen, 447 m asl, since 2011 (Fjeldheim and Barfod, 2013; Stranden and Ree, 2014). The station encompasses a temperature and humidity sensor (Campbell CS215), rain gauge (OTT-pluvio), wind sensor (RMYoung), snow scale (Møen 2525), snow pillow as well as a snow depth sensor (Campbell SR50AT). Ottar Husum conducts manual control measurements for snow depth and density to check the data quality of existing instrumentation at Anestølen weather station at 4-to-6-week interval throughout the winter when the Anestølen weather station can only be accessed with skis.

We back-calculate the historical account of maximum runouts and the observed snow avalanches with the numerical simulation programs

RAMMS::Avalanche (Christen et al., 2010) and RAMMS::Extended (Glaus et al., 2023). Whilst we only show five scenarios, a total of 50 simulation runs have been performed to test sensitivity to the input data and parameters. For the modelling, we used a DTM from 2016 based on airborne LiDAR data. Resolutions of the calculation grid between 1 and 10 m were tested, while all presented results have 5 m resolution. As we struggled to reproduce long enough runouts north of the fan where the core transect is located, we edited the DTM to remove parts of the fan and gully to account for potential topographic changes since early Holocene. These scenarios did not result in markedly longer runouts or better fitting runout patterns and are not shown here. In RAMMS::Avalanche, we model with standard Voellmy parameters (μ=0.2, ξ=2000) as well as with variable Voellmy parameters for medium and large avalanches with 100 or 300 year return periods respectively (altitude limits adjusted to Norwegian conditions). The resulting Voellmy parameters for medium and large scenarios range from 0.20 to 0.37 and 0.16 to 0.30 respectively for the Coulomb-type friction (μ) as well as from 1100 to 2500 m s^{-2} and 1200 to 3000 m s^{-2} respectively for the viscous turbulent friction coefficient (ξ). In RAMMS::Extended the initial frictional parameters (μ_0, ξ_0 and N_0) are determined based on preset values representing 10, 30 and 100 year return periods. Depending on temperature and liquid water content (LWC), Coulomb-type and turbulent friction are then calculated for each time step. RAMMS::Extended is sensitive to input of temperature and LWC (Glaus et al., 2023; Miller et al., 2023). As we lack sufficient control on the timing of avalanches in 2012 and 2015 and certainly for the historical sediment record, we generalize release conditions into a dry scenario (snow temperature -5°C, snow density at release 200 kg m^{-3}, at deposition 450 kg m^{-3}, LWC_0 = 0 mm m^{-2}) and wet scenario (snow temperature 0°C, snow density at release 300 kg m^{-3}, at deposition 450 kg m^{-3}, LWC_0 = 1 mm m^{-2}). The snow depth and temperature had an adjustment rate of 0.03 m 100 m^{-1} and 0.3°C 100 m^{-1}, respectively. Whilst RAMMS::Extended allows for the simulation of the interaction between core and powder cloud, for simplicity we have chosen to focus on the flowing part.

As frozen water bodies are commonly used as motorways in the high-Arctic, bearing capacity of ice has been a concern for engineers and we may borrow some of the employed concepts (e.g. Hertz, 1884; Ashton, 1986; Sodhi, 1995). In the elastic plate theory, the characteristic length *L* or radius of the deflected ice area:

$$L^4 = \frac{Eh^3}{12(1-\nu^2)\rho_w g} \quad (1)$$

can be expressed with the elastic modulus *E*, ice thickness *h*, Poisson's ratio *v*, density of water *ρ* and gravitational constant *g*.

The failure or ultimate load can then be determined with a semi-empirical equation:

$$P_u = 1.25\,(1 + 1.68\alpha)\,\sigma_f h^2 \quad (2)$$

with σ_f which is the flexural strength of an ice sheet when the bottom is in tension and the maximum momentum α which can be calculated as load contact radius divided by the characteristic length:

$$\alpha = {}^{r}/_{L} \quad (3)$$

4. RESULTS

In the following, we present the historical and meteorological account of snow avalanches which hit the lake ice of Anestølsvatnet in the past decade and the back-analysis of the observed avalanche paths and runouts with the simulation programs RAMMS::Avalanche and RAMMS::Extended.

4.1 Historical snow avalanches on lake ice

Historical accounts of snow avalanches hitting lake Anestølen are scarce as it can only be accessed by ski in wintertime. Ottar Husum who skis into the valley regularly to measure snow depth and density has observed two larger noteworthy snow avalanches since 2011.

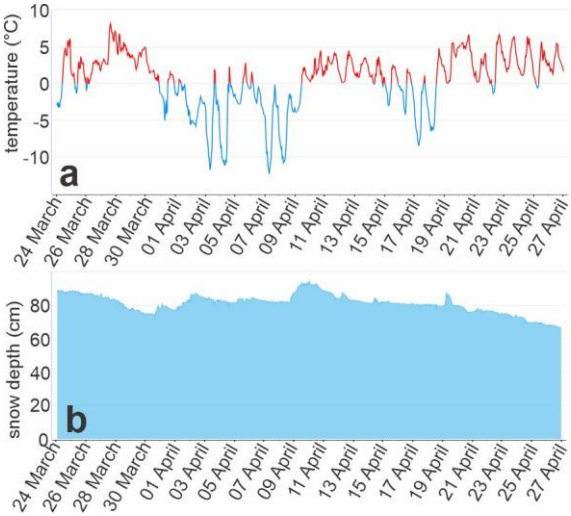


Figure 2: Hourly temperature (**a**) and snow depth record (**b**) at Anestølen from March 24th to April 26th 2012 when the snow avalanche debris was observed

Figure 1b shows avalanche debris on the lake ice observed on April 26th, 2012. On his prior visit on March 24th, 2012, the avalanche had not occurred yet. Temperature and snow depth records for the time of potential avalanche release are

shown in Figure 2. Together with information on the snow stability of the forecasting service, which suggest stable conditions end of March and frequent wet loose snow avalanches from mid-April, the most likely period for slab avalanche release is during snowfall on April 8-9th and the following day with rising temperatures.

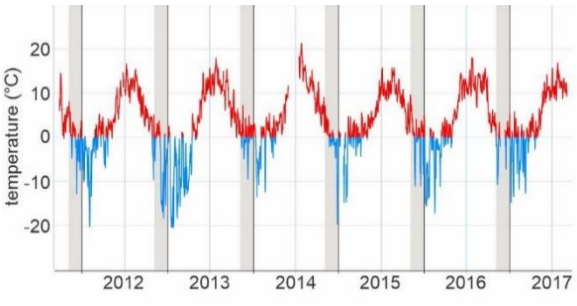


Figure 3: Temperature record at Anestølen from autumn 2011 until summer 2017

Three years later in 2015 Ottar Husum recalls observing a different avalanche-on-lake-ice end member. Unfortunately, the exact date of occurrence is unknown as the photos that he took at the time are now unavailable. Whilst it occurred in the same avalanche track, Storeskreda (Figure 1a), it had markedly different characteristics than the one observed in 2012. The 2015 avalanche had a much shorter runout as snow had piled up on the ice at proximity to the lake shore where it had caused the lake ice to break. The impact of the avalanche caused numerous shore-parallel fractures extending all the way to the opposite lake shore. According to Ottar Husum these cracks resembled ogives on a glacier.

The temperature record from seasons 2011/12 to 2016/17 (November-December highlighted with light grey background in Figure 3), suggest suboptimal conditions for lake ice formation in the 2014/15 season. Unfortunately, there were some days with lacking temperature data in January, but a near-by station suggests January 6-18 to have had daily temperature close to and above 0 °C. There were no sustained temperatures below -5 °C from October 2014 to January 2015, but temperatures were below zero for large parts of December when a meter of snow accumulated.

4.2 Back-analyses of observed avalanche and runouts in RAMMS::Avalanche

Scenario 1: We delineated the starting area at 1175-1250 m asl on Oksli mountain (Figure 4a) with 1.5 meter starting depth, resulting in an estimated release volume of 33 880 m^3. Variable Voellmy parameters correspond to the large scenario as described in the methods. The deposition resulting from this model scenario is shown in Figure 4a, the maximum velocity in Figure 4b. Despite being a medium-sized avalanche with low

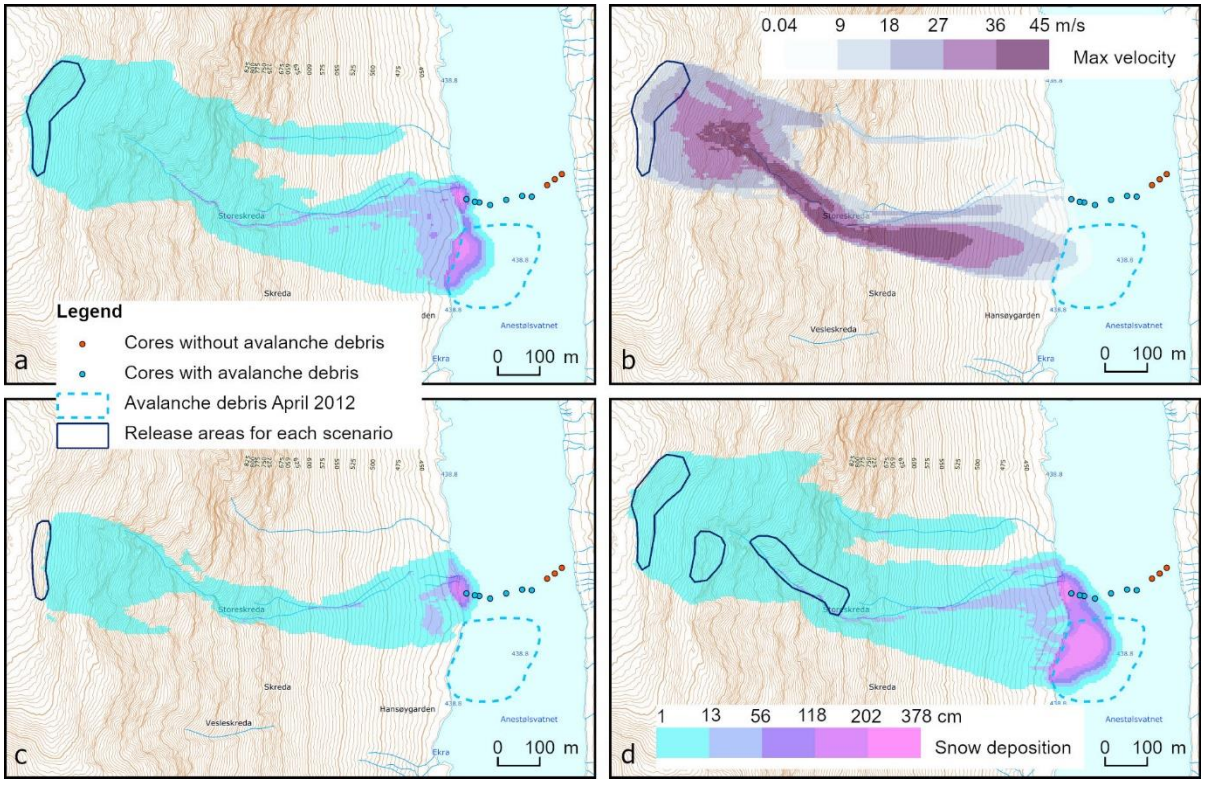


Figure 4: Three scenarios modelled in RAMMS::Avalanche: (**a**) snow deposition and (**b**) maximum velocity for scenario 1, (**c**) snow deposition for scenario 2 and (**d**) snow deposition for scenario 3

friction values the runout on the lake does not match the observed runout from the 2012 avalanche nor the maximum reach of snow avalanche debris in the sediment cores. At this size the snow debris is almost equally distributed over the northern and southern part of the fan.

Scenario 2: Here we model a small avalanche starting at 1200-1225 masl on Oksli with 1 meter starting depth, resulting in an estimated release volume of 8427 m^3. Variable Voellmy parameters correspond to the medium scenario as described in the methods. This small avalanche scenario results in a northern path over the fan but is far from inferred historical runout lengths based on sediment cores (Figure 4c). This scenario certainly does not reflect the 2012 avalanche adequately.

Scenario 3: This scenario consists of the same starting area (1175-1250 m asl on Oksli) as in scenario 1, in addition to two secondary starting areas with 10 and 24 s delay, at 1050-1125 and 750-950 m asl respectively. All of these were set to 1 meter starting depth, resulting in a total starting volume of 56 281 m^3 which is approaching the large avalanche category. The runout length is still around 50 meters short compared to the avalanche debris observed in 2012, and the modelled area of deposition is much wider (Figure 4d).

The flow becomes channelized through the steepest passage between 1100 and 650 m asl. It seems that the speed acquired at 750-700 m asl just before reaching the fan apex is crucial for how the snow is distributed further over the fan. Smaller avalanches or avalanches with lower release areas may have their focus of deposition beyond the northern fan, while larger, faster avalanches seem to shoot out of the channel at 750-700 m asl resulting in deposition beyond the southern reaches of the fan.

4.3 Back-analyses of observed avalanche and runouts in RAMMS::Extended

Scenario 4: This is a dry scenario with starting area at 1175-1250 m asl (same as scenario 1) and 0.7 meter starting depth, giving an estimated release volume of 16 156 m^3. The initial friction parameters are chosen for an avalanche with 10-year return period (μ_0 = 0.55, ξ_0 = 1800 m s^{-2}, N_0 = 200 Pa). This scenario matches the observed runout for the 2012 avalanche well (Figure 5a).

Scenario 5: This is a wet scenario for a medium-sized (1m starting depth, 26 585 m^3 release volume) slab avalanche starting in the gully from 750-950 m asl. Return period is set to 100 years (μ_0 = 0.42, ξ_0 = 1900 m s^{-2}, N_0 = 100 Pa). Even though the avalanche starts in warm snow, it does not produce meltwater and no lubrication occurs resulting in piles of snow by the lake shore (Figure 5b).

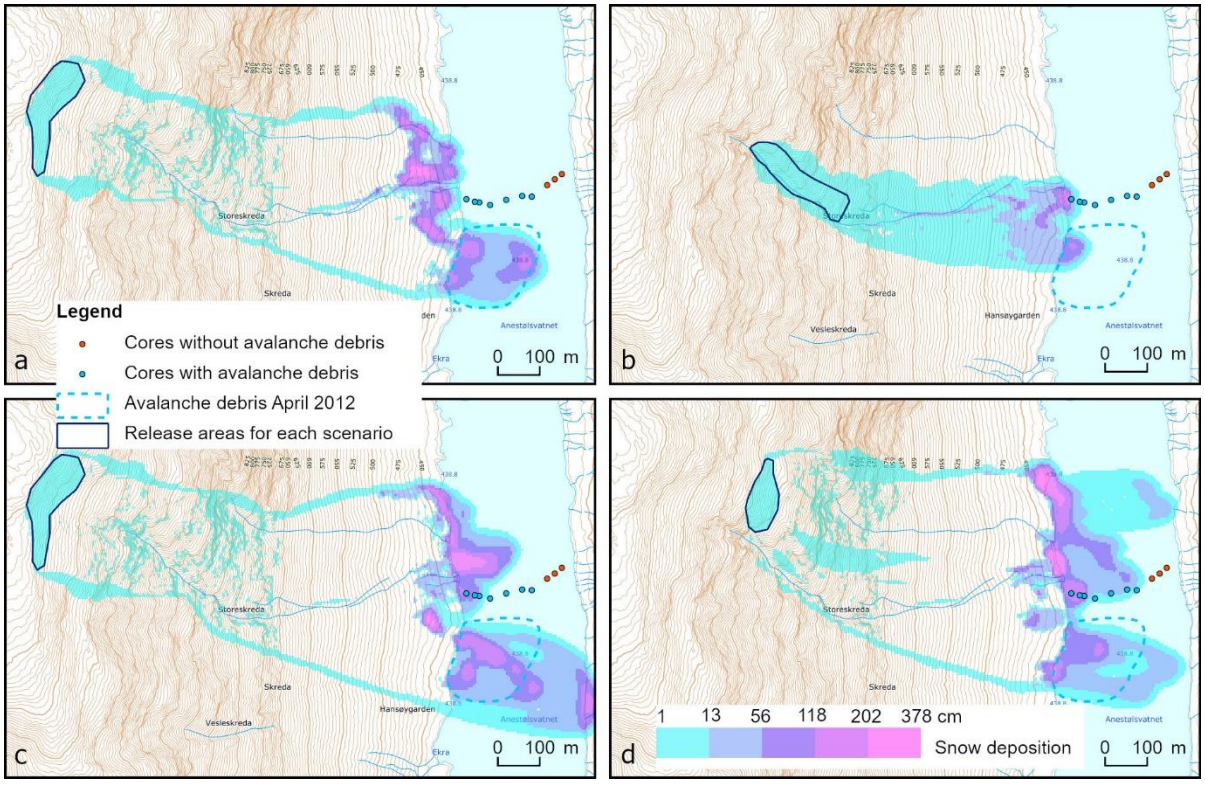


Figure 5: Four scenarios modelled in RAMMS::Extended showing snow deposition for (**a**) scenario 4, (**b**) scenario 5, (**c**) scenario 6 and (**d**) scenario 7

Scenario 6: Starting area at 1175-1250 m asl (same as scenario 1 and 4) and 1 meter starting depth, give an estimated release volume of 23 080 m^3 in this dry scenario. The initial friction parameters correspond to a 100-year avalanche (μ_0 = 0.42, ξ_0 = 1900 m s^{-2}, N_0 = 100 Pa). This simulation run suggests that snow debris from a medium-sized avalanche can reach all the way across the lake and climb onto the eastern shore at the southern reaches of the fan (Figure 5c).

Scenario 7: Small starting area at 1000-1050 m asl with 1 meter starting depth (13 023 m^3 release volume) and 100-year return period (μ_0 = 0.42, ξ_0 = 1900 m s^{-2}, N_0 = 100 Pa) creates this extensive deposition in a dry slab avalanche scenario (Figure 5d). This is considered amongst the simulation runs with better fit regarding observed maximum runout at the northern reaches of the fan based on the sediment core transect.

Despite exclusively modelling small- to medium-sized release scenarios, the runouts are markedly longer than those modelled with RAMMS::Avalanche, even reaching the opposite lake shore in scenarios 6 and 7 (Figures 5c and 5d).

5. DISCUSSION

Whilst direct observations of snow avalanches on Lake Anestølen by Ottar Husum are valuable, time control is relatively poor, in particular for the 2015 avalanche. Unfortunately, Sentinel 1 and 2 missions were not operational at the time and available satellite data does not allow for recognition of avalanche debris on the lake ice in this narrow valley. Nevertheless, the analysis of weather conditions prior to the two largest snow avalanches in recent years give some useful insights. Within the month of potential occurrence of the 2012 avalanche, April 8-10th stand out as most likely period of release, but only 10 cm of snow accumulated at the Anestølen weather station and wind speeds were below 3 m s^{-1} these days. In the time window of question weakening of a deeper weak layer due to warming could have been just as likely as loading by precipitation and/or wind. So unfortunately, the trigger remains unresolved.

The season 2014/15 clearly stands out with an autumn which promoted the formation of weak lake ice. Temperatures were unusually mild in October and November but between 0 °C and -5 °C in December. In this period, a meter of snow accumulated. Snow falling on thin lake ice acts as in insulator and hinders the formation of thick and strong columnar ice, also in colder periods later in winter (Leppäranta, 2015). Therefore, it is not surprising that the avalanche which punched through the lake ice was observed in 2015. The presented semi-empirical formula for failure load can only be applied for ice of good quality, 30 cm of rotten ice may have lost all its bearing capacity (Fransson, 2009).

Maximum pressures calculated in the RAMMS scenarios presented above vary from 5 to 420 kPa at the lake shore. Peak pressures calculated with RAMMS::Avalanche are 5 kPa (scenario 2), 85 kPa (scenario 1) and 110 kPa (scenario 3). Pressures for the RAMMS::Extended scenarios are generally higher and range from 60 kPa (scenario 5) over 240 kPa (scenario 4), 320 kPa (scenario 7) to 420 kPa (scenario 6). In the following, we consider whether such pressures are sufficient to break through lake ice.

When loaded on a short time scale (1-2 min and less) ice shows elastic behavior, on very short time scales (seconds) it behaves in an elastic-brittle fashion whilst the long-term response is viscous-plastic (Leppäranta, 2015). Uniaxial compressive brittle strength of lake ice ranges within 1-10 MPa with highest values for cold, fine-grained ice (Michel, 1978). Shear strength depends primarily on the strain rate and not much on temperature with values in the range of 0.5-1.5 MPa (Leppäranta, 2015). Based on comparison of these values with maximum pressures calculate in RAMMS, brittle failure on a very short timescale of seconds becomes unlikely. When considering whether the break-through load can be reached elastically, the limiting factor is that it is difficult to determine the correct impact radius and that avalanches are not static but dynamic loads. Assuming the load to be static, we use the semi-empiric elastic plate theory equation (Hertz, 1884) for some quick calculations. With fixed input values for the elastic modulus E = 9 GPa, Poisson's ratio v = 0.33, density of water ρ_w = 1000 kg m^3 and gravitational constant g = 9.81 m s^2, we varied the flexural strength of lake ice σ_f = 0.5-1.5 MPa, lake ice thickness h = 0.05-0.30 m and impact radius r =1-5 m. The results suggest that scenario 2 will not break the ice whilst all other scenarios have the potential to break the ice depending on the chosen ice thickness and flexural strength.

RAMMS::Extended produced markedly longer runouts and different depositional patterns for comparable scenarios. We have only modelled the flowing part of the avalanche, so powder-core-interactions can be ruled out as explanation (e.g. Bartelt et al., 2015). Snow entrainment or snow erodibility incorporated in RAMMS::Extended is treated as a fully plastic collision and is an important source of random kinetic energy (or granular temperature) thus dissipating this heat and raising the temperature in the core (Bartelt et al., 2018). Mean avalanche temperature is introduced in RAMMS::Extended and plays a crucial role for

the representation of avalanche dynamics; it governs the meltwater generation and dry-wet-transitions are in turn accounted for with a water-dependent Voellmy-type friction law (Glaus et al., 2023). Therefore, the frictional parameters evolve through the simulation and are temperature-dependent: the closer to 0 °C the release temperature, the less fluidized the avalanche and the shorter the runout. If, however, generated temperatures are warm enough to create meltwater through frictional heating, lubrication may lead to longer avalanche runout. This is the case in scenarios 4 and 6 (Figures 5a and 5c) where meltwater is produced on the southern part of the fan just before entering the lake ice. This accounts for much longer runouts over the ice than for comparable scenarios in RAMMS::Avalanche. When snow entrainment is mimicked by the inclusion of secondary starting areas in RAMMS::Avalanche as in scenario 3, the maximum runout occurs beyond the southern reaches of the fan and maximum runouts observed from the core transect cannot be reproduced (Figure 4d).

No meltwater is produced in scenario 7 (Figure 5d), so lubrication cannot explain the observed runouts all the way across the lake. In RAMMS::Extended the modelled avalanches sustain their high velocities over the fan, whereas they slow down shortly after the fan apex in RAMMS::Avalanche. We await discussions at the conference for clarifications on why this might be the case.

6. CONCLUSIONS

We present indirect and direct observations of two end members of snow avalanches lake ice interaction: (i) snow avalanches hitting lake ice and melting out in spring and (ii) snow avalanches breaking through lake ice upon impact. Attempts to back-analyze observed and inferred runouts in conventional RAMMS::Avalanche are not successful, while RAMMS::Extended is able to reproduce different observations satisfactory. Snow entrainment and meltwater production can explain large differences in the modelled runout and depositional pattern. In RAMMS::Avalanche the momentum on the fan apex is crucial for the path the avalanche takes over the fan.

ACKNOWLEDGEMENT

Thanks to Kristian Vasskog (UiB), Marthe Gjerde (HVL) and bachelor students Jonas Kimerud, Therese Hansen, Julie R. Bergaas, Marta, L. Jahnsen and Håkon Skjørestad for their contributions to the sedimentological study. Ottar Husum kindly provided information about his regular observation trips to Anestølen.

REFERENCES

Ashton, G. D.: River and lake ice engineering, Water Resources Publication1986.

Bartelt, P., Buser, O., Valero, C., and Bühler, Y.: Configurational energy and the formation of mixed flowing/powder snow and ice avalanches, Annals of Glaciology, 179–188, https://doi.org/10.3189/2016AoG71A464, 2015.

Bartelt, P., Christen, M., Bühler, Y., Caviezel, A., and Buser, O.: Snow entrainment: Avalanche interaction with an erodible substrate., International Snow Science Workshop Proceedings, Innsbruck, 716-720,

Bergaas, J. R., Jahnsen, M. L., and Skjørestad, H.: Sedimentær signatur etter snøskred i innsjøavsetninger fra Anestølsvatnet, Sogn, Bachelor thesis, Western Norway University of Applied Sciences, Sogndal, 2018.

Christen, M., Kowalski, J., and Bartelt, P.: RAMMS: Numerical simulation of dense snow avalanches in three-dimensional terrain, Cold Regions Science and Technology, 63, 1-14, https://doi.org/10.1016/j.coldregions.2010.04.005, 2010.

Fjeldheim, H. L. and Barfod, E.: Filefjell og Anestølen forskningsstasjon - Evaluering av måledata for snø, sesongen 2011/2012, Oslo, 2013, 2013.

Fransson, L.: Ice handbook for engineers, 1.2, Luleå University of Technology2009.

Glaus, J., Jones, K. W., Bühler, Y., Christen, M., Ruttner-Jansen, P., Gaume, J., and Bartelt, P.: RAMMS::EXTENDED - Sensitivity analysis of numerical fluidized powder avalanche simulations in three-dimensional terrain, International Snow Science Workshop Proceedings, Bend, 795-802,

Hertz, H.: Über das Gleichgewicht schwimmender elastischer Platten, Annalen der Physik, 258, 449-455, 1884.

Kimerud, J. and Hansen, T.: Karakterisering av skredsignaturer basert på innsjøsedimenter fra Anestølsvatnet Sogn, Bachelor thesis, Western Norway University of Applied Sciences, Sogndal, 2018.

Leppäranta, M.: Freezing of lakes and the evolution of their ice cover, Springer2015.

Michel, B.: A mechanical model of creep of polycrystalline ice, Canadian geotechnical journal, 15, 155-170, 1978.

Miller, A. D., Redpath, T. A. N., Sirguey, P., Cox, S. C., Bartelt, P., Bogie, D., Conway, J. P., Cullen, N. J., and Bühler, Y.: Unprecedented Winter Rainfall Initiates Large Snow Avalanche and Mass Movement Cycle in New Zealand's Southern Alps/Kā Tiritiri o te Moana, Geophysical Research Letters, 50, e2022GL102105, https://doi.org/10.1029/2022GL102105, 2023.

Rüther, D. C., Røthe, T. O., Vasskog, K. and Gjerde, M.: Mass movement signature in lacustrine sediments at Anestølen, Western Norway, unpublished manuscript.

Sodhi, D. S.: Breakthrough loads of floating ice sheets, Journal of cold regions engineering, 9, 4-22, 1995.

Stranden, H. B. and Ree, B. L.: Filefjell og Anestølen - Evaluering av måledata for snø, sesongen 2012/2013, Oslo8241010230, 2014.

Aa, A. R., Bondevik, S., and Sønstegaard, E.: Holocene debris flows and snow avalanches in Anestølsdalen, western Norway - recorded from lake deposits and colluvial fans, Norwegian Journal of Geology, 102, 2022.